

## Pseudo-polymorphism and crystalline transition of magnesium stearate

Yasutaka Wada and Takashi Matsubara

*Shionogi Research Laboratories, Shionogi & Co, Ltd., 5-12-8 Sagisu, Fukushima-ku, Osaka 553 (Japan)*

(Received 12 June 1991)

### Abstract

The polymorphic characteristics of 23 commercial batches of magnesium stearate obtained from various suppliers were examined by various methods. Differential scanning calorimetry (DSC) was found to be the most useful for distinguishing the different forms. The magnesium stearate samples examined were classified into six forms based on their DSC curves. These forms showed different sensitivities to heat and moisture. Reversible transition of one form to another was detected on treatment of the samples with or without water molecules, with crystal water playing an important role in the form transition.

### INTRODUCTION

Magnesium stearate is most widely used as a lubricant in the process of compressing tablets and filling capsules, mainly due to its ability to decrease friction. Magnesium stearate is alkaline and hydrophobic, and can coat the surface of powder particles [1]. If excess lubricant is used or the mixing time is too long, problems arise, such as a decrease in the drug content [2], a decrease in the tablet hardness [3–9], an increase in the disintegration time [5–7,10], an increase in the dissolution time [11,12] or a decrease in the bioavailability [13]. Therefore, only the minimum effective amount should be used.

Since the discovery of the lubricant property of commercial magnesium stearate by Hansen et al. [14], the polymorphism of the compound and its relationship to the lubricating properties have been studied by Müller and Steffens [15], Steffens et al. [16], Miller et al. [17], Colombo and Carli [18], Dansereau and Peck [19], Ertel and Carstensen [20] and Ikonen et al. [21]. It has been suggested that gas molecules also contribute to the lubricating properties [22]. Pure magnesium stearate is difficult to obtain because it is insoluble in water and organic solvents and because unreacted materials contaminate its matrix. Thus, although its polymorphic properties have attracted much attention, little is known about them. We have studied the polymorphic characteristics of magnesium stearate by various methods, and

have found that differential scanning calorimetry is the most useful method for detecting the polymorphism. Here we also demonstrate the importance of crystal water in the polymorphic character of magnesium stearate.

## EXPERIMENTAL

### *Materials*

Twenty-three batches of magnesium stearate were obtained from Taihei Chemical Co., Ltd. (Taihei), Wako Pure Chemical Industries Ltd. (Wako), Nacalai Tesqu, Inc., formerly Nakarai Chemicals, Ltd. (Nacalai), Kanto Chemical Co., Ltd. (Kanto Chem.) and Tokyo Kasei Kogyo Co., Ltd. (Tokyo Kasei). The samples were stored at room temperature in sealed containers until use. Samples were prepared as follows.

*Intact.* Magnesium stearate samples purchased from distributors were used for the experiments without further treatment.

*Washed.* Magnesium stearate (3 g) was suspended in 100 ml of acetone, stirred for 10 min and filtered twice. The resulting sample was dried in air.

*Dried.* The sample was kept for about 3 weeks in a reduced desiccator over phosphorous pentoxide.

*Stored (1).* The sample was stored in a sealed container at 60 °C for 3 months.

*Stored (2).* The sample was wetted with acetone and water was added to the sample container. With the suspension maintained at 60 °C, acetone evaporated from the container to the atmosphere and water was added at about the same time. The suspension was stored in the sealed container at 60 °C for 1 month. The resulting sample was dried in air just before the experiments.

*Held (1).* The sample pan containing magnesium stearate was held in the DSC at a definite temperature for 1 h and then cooled to room temperature.

*Held (2).* The sample pan was held in the DSC at a definite temperature for 1 h with addition of water, using a procedure developed by Suzuki et al. [23], and then cooled to room temperature.

### *Determination of thermal properties*

The thermal properties of the sample were determined using two thermal analysis systems, employing two thermogravimeters (TG) and two power-compensated differential scanning calorimeters (DSC). One system was the TG–DSC model CN8089 of Rigaku Corp. (Tokyo, Japan) which is called TG-1 and/or DSC-1, and the other system was the Perkin–Elmer

Series 7 model, called TG-2 and/or DSC-2. DSC instrumental analyses were carried out as follows.

(1) Most of the measurements were performed under the following conditions: sample weight, 5 mg; sample pan, aluminum, 2.5 mm × 5 mm i.d.; temperature range, 38–220 °C; heating rate, 5 °C min<sup>-1</sup>; flow rate of nitrogen gas, 220 ml min<sup>-1</sup>.

(2) In some experiments, samples heated in this way were then cooled to 38 °C at the rate of 5 °C min<sup>-1</sup>.

(3) Samples were put on dry ice and stored for 1 day immediately after the sample pans had been heated to the set temperature (80–220 °C). The DSC pattern was then measured using the above procedure (1).

TG examination with TG-1 was carried out under the following conditions: sample weight, 10 mg; sample pan, aluminum, 5 mm × 5 mm i.d.; temperature range, 25–220 °C; heating rate, 5 °C min<sup>-1</sup>; flow rate of nitrogen gas, 50 ml min<sup>-1</sup>. The conditions with TG-2 were the same as for TG-1, except that the sample weight was 5 mg.

### *Measurement of melting points*

The sample melting point was measured according to Method 1 of Pharmacopoeia of Japan, Eleventh Edition (JPXI).

### *Determination of physico-chemical properties*

Particle size and specific surface area were measured with a Sub-Sieve Sizer apparatus (Fisher Scientific Corp., Pittsburgh, Pa., USA) at a porosity of 0.575. Moisture contents were measured by the Karl Fisher method and magnesium contents by oxygen flask combustion–ion chromatography. To measure the composition ratio of fatty acid, the sample was destroyed by diluted hydrochloric acid in ether, and the ether layer was vaporized. The residue containing fatty acid was dissolved in acetonitrile and labeled with 3-bromomethyl-6,7-dimethoxy-1-methyl-2(1H)-quinoxalinone (Br-DMEQ) [24]. The Br-DMEQ derivatives of fatty acid were separated and detected with a Shimadzu high-performance liquid chromatography LC-6A equipped with a cartridge column model Capcell Palc C18 SG (150 mm × 4.6 mm i.d., Shiseido, Tokyo, Japan) at the UV wavelength of 254 nm with 93% aqueous methanol as the mobile phase.

### *Scanning electron microscopy (SEM)*

Microscopic observations of the samples were made using a Jechnics scanning electron microscope JSM-840A.

### *X-ray powder diffractogram (X-ray)*

A Rigaku X-ray powder diffraction analyzer RINT-1400 with a monochromator and controlled heat attachment was used to record the X-ray diffractograms. The examination conditions were as follows: Cu  $K\alpha_1$  radiation;  $\lambda$ , 1.54056 Å, 60 kV, 200 mA; DS, 0.3 mm; SS, 0.5 deg; scanning speed, 4 deg  $\text{min}^{-1}$ , angle of data sampling  $2\theta$ , 1–30 deg, interval of sampling, 0.02 deg, measured temperature point, before and after the DSC peak.

### *Infrared absorption spectroscopy (IR)*

IR spectra were measured by the potassium bromide tablet method with a JASCO IR spectrometer A-702.

## RESULTS AND DISCUSSION

### *Thermal properties*

#### *DSC*

TG–DSC curves of 23 intact samples of magnesium stearate were measured with TG–DSC-1; six different DSC patterns were found, as indicated in Fig. 1. We arbitrarily classified the samples into six groups: Mg-st A, B, C, D, E and F, depending on their characteristic patterns. Under our survey conditions, 14 of the 23 samples were classified as Mg-st A, three as Mg-st B, two as Mg-st C, one as Mg-st D, two as Mg-st E and one as Mg-st F. Further experiments were then carried out using a typical batch of each form.

Mg-st A has peaks at 104, 127 and 202 °C, and an exothermic peak at about 174 °C. The exothermic peak or exothermic performance in the DSC curve was also detected in Mg-st B, C and D. Comparing the DSC curves below 150 °C, shows that Mg-st B has a peak at 118 °C in addition to the Mg-st A peaks at 104 and 127 °C. Mg-st B has a curve similar to that of Mg-st A with a peak at 118 °C; and Mg-st D has a similar curve with another peak at 80 °C. Mg-st C seemed to be a mixture of Mg-st B and Mg-st E because its DSC curve is similar to a combination of Mg-st B with Mg-st E.

The DSC curve of Mg-st A below 150 °C is identical to the “Undried” curve reported by Miller et al. [17] and to “Form A” of Ertel and Carstensen [20(a)]. The DSC curve of Mg-st E is similar to “K” of Müller [15(a)] who used differential thermal analysis. The other DSC curves have hitherto unknown forms.

Mg-st A has a broad exothermic peak above 160 °C, and Mg-st B, C and D show similar exothermic phenomena with the curve falling below the

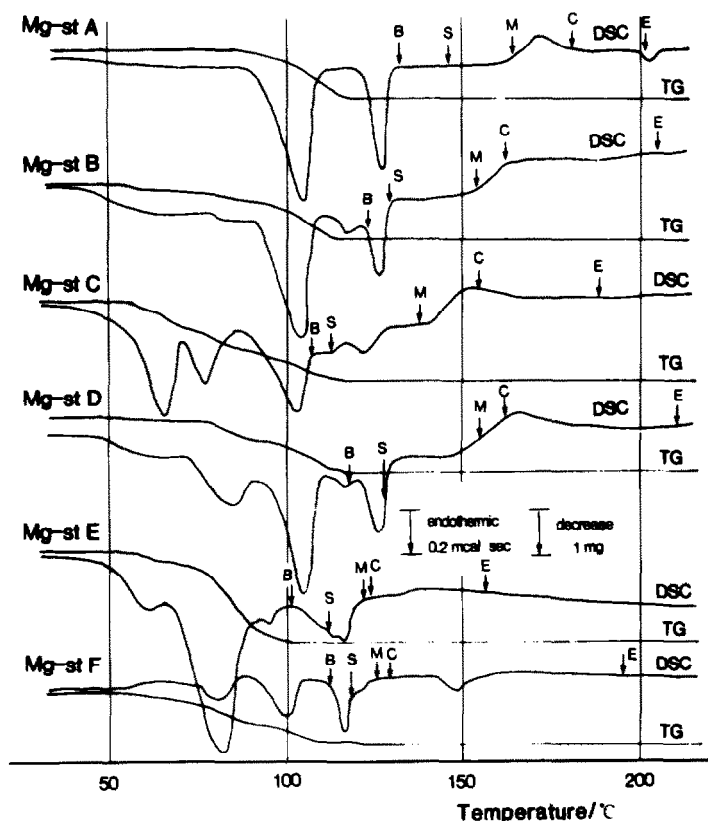


Fig. 1. TG-DSC curves of various forms of magnesium stearate obtained by measurement with DSC-TG-1. Melting points of the same forms of magnesium stearate were also determined by the JPXI method 1 and the temperature is indicated on the DSC curve by the arrow. Heating rate,  $5^{\circ}\text{C min}^{-1}$ ; sample weight, 5 mg (DSC) and 10 mg (TG); sample pan, aluminum open pan; standard,  $\alpha$ -alumina; atmosphere, nitrogen gas. Arrowed letters: B, beginning of melting; S, sintering point; M, meniscus point; C, collapse point; E, end of melting.

base line. Many investigators have reported on the DSC properties of magnesium stearate, but no one has reported a DSC curve above  $150^{\circ}\text{C}$ . Thus, attention was focused on the exothermic performance of the samples. When Mg-st A was mixed with 20% or 40% basic magnesium carbonate, the broad exothermic peak above  $174^{\circ}\text{C}$  gradually increased with an increase in the magnesium carbonate concentration. Mixing Mg-st B, C or D with 20% basic magnesium carbonate led to the appearance of a sharp exothermic peak from the exothermic phenomena with curves falling below the base line. Therefore it seems likely that impurities in the samples are reacting at these temperatures, giving exothermic peaks on the DSC curve.

The Mg-st F sample is known to be a poor lubricant. DSC was useful for clearly differentiating among the forms including Mg-st F.

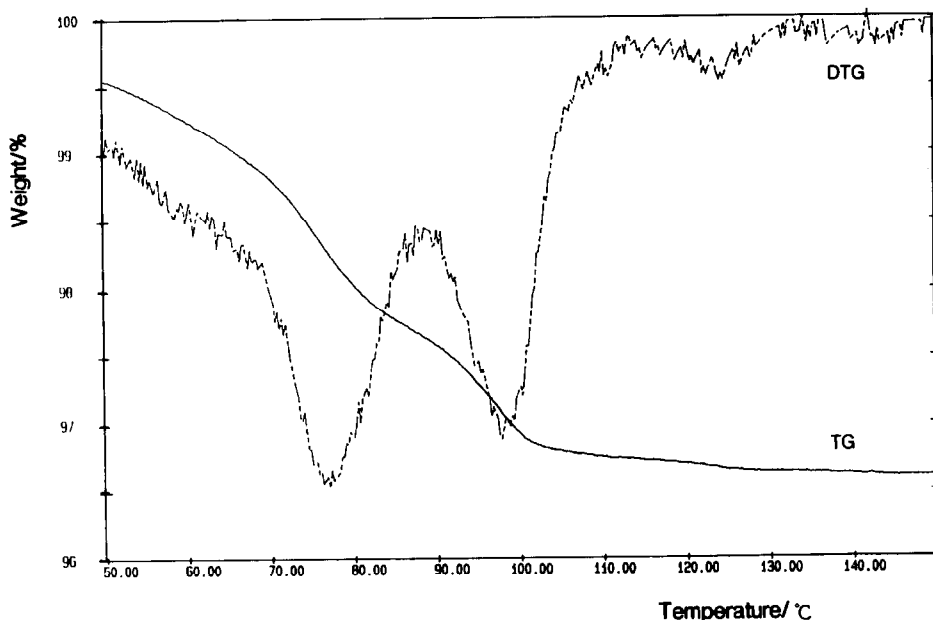


Fig. 2. TG-DTG curve of Mg-st F measured by TG-2.

### TG

Increasing the temperature led to a fall in the TG curves of Mg-st A and B representing 1.5 mol of water associated with the appearance of the DSC peak at 104 °C (Fig. 1). However, the weight loss of Mg-st C is a three-step process: about 0.5 mol of water being lost at the DSC peak of 61 °C, 0.5 mol at the 75 °C peak and 0.5 mol at the 101 °C peak. Mg-st D shows desorption of water at 80 °C with loss of 1.5 mol water at 103 °C. Mg-st E shows desorption of water at 58 °C with loss of 2 mol of water at 83 °C.

The TG curve and the derivative thermogravimetry (DTG) curve of Mg-st F are shown in Fig. 2; Fig. 3 shows the expanded curve.

The TG curve of Mg-st F reveals a step-wise loss of water: above 1 mol water at 78 °C and another 1 mol water at 99 °C, with a weight loss of 0.09% at 116 °C. TG curve patterns of Mg-st A, B, C, D and E show desorption of water at a few of the low temperature DSC peaks, remaining stable at the highest DSC peak. In contrast, there is a slight fall in the TG curve of Mg-st F at the temperature of the highest DSC peak (Fig. 3).

From these results, the maximum peak temperature, the initial DSC peak temperature, the moles of water loss per mole of sample and the enthalpy per gram of sample were determined, as shown in Table 1.

### *Relationship between DSC curves and melting points*

According to the JPXI melting point test, the beginning of melting (B), the sintering point (S), the meniscus point (M), the collapse point (C) and

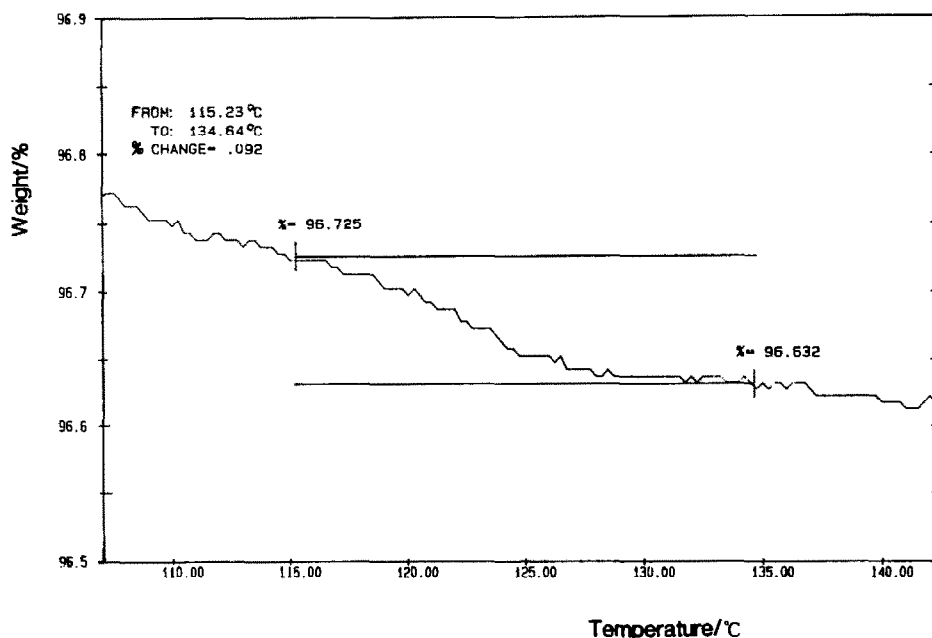


Fig. 3. Enlarged TG curve of Fig. 2.

the end of melting (E) of the samples were observed and are shown as arrows in Fig. 1. Each sample has a wide temperature range from the beginning to the end of melting. Mg-st E, having no exothermic peaks above 160 °C has the most narrow melting point range, suggesting the lowest levels of impurities. Not every arrow coincided with every initial temperature of the DSC peaks, but the arrows for the meniscus point are roughly coincident with the initial point of the peak. From observations of sample pans when the heating attachment was removed from the DSC apparatus, at around the meniscus point the sample turned from a white powder to a transparent liquid and the volume diminished. The results shown in Fig. 1 indicate no correlation between the melting point, defined as the end of melting in JPXI, and the DSC curve of the samples.

#### *Physico-chemical properties of various magnesium stearate samples*

Particle size, specific surface area, bulk density, moisture content, magnesium content and ratio of fatty acid composition in the various magnesium stearate samples investigated are shown in Table 2.

Because the weight loss determined by TG is approximately the same as the moisture content of the sample, it was recognized that the weight loss is dependent on the desorption of water, except for the 116 °C DSC peak of Mg-st F.

TABLE 1

Thermal properties of various forms of magnesium stearate

Form	$T_p$ (K) <sup>a</sup>	$T_1$ (K) <sup>b</sup>	$\Delta W$ (mol) <sup>c</sup>	$\Delta h$ (J g <sup>-1</sup> ) <sup>d</sup>
Mg-st A	377.4	364.1	1.5 +	11.27 ± 0.48
	400.1	396.4	-	4.47 ± 0.36
	446.9	434.0	-	-2.70 ± 0.64
	475.4	473.0	-	0.08 ± 0.02
Mg-st B	376.6	366.4	1.5 +	7.74 ± 0.42
	391.1	387.8	-	0.92 ± 0.07
	400.5	397.0	-	3.01 ± 0.26
Mg-st C	334.5	322.6	0.5 +	7.37 ± 0.69
	347.9	343.3	0.5	5.09 ± 0.44
	373.8	367.7	0.5	6.84 ± 0.45
	384.8	380.2	-	2.70 ± 0.28
	397.5	394.3	-	1.33 ± 0.11
Mg-st D	353.6	342.4	+	5.72 ± 0.23
	376.4	366.5	1.5	9.48 ± 0.76
	391.5	386.5	-	0.99 ± 0.15
	400.2	397.1	-	3.06 ± 0.14
Mg-st E	331.7	322.2	+	3.01 ± 0.23
	356.5	341.9	2	21.18 ± 1.09
	371.4	369.1	-	2.48 ± 0.20
	392.2	380.2	-	5.08 ± 0.11
	395.3	392.5	-	0.43 ± 0.06
Mg-st F	351.5	345.4	1+	1.96 ± 0.07
	372.2	364.5	0.5	2.38 ± 0.24
	389.5	386.7	+	2.59 ± 0.12
	422.3	419.5	-	0.78 ± 0.11

<sup>a</sup> Maximum peak temperature.<sup>b</sup> Initial peak temperature.<sup>c</sup> The numbers indicate the loss of moles of water per mole of magnesium stearate, and + indicates the loss of a fragment.<sup>d</sup> Mean ± S.D. in 3 samples.

From the chemical formula of magnesium stearate, the magnesium content is 4.11%. The magnesium content of Mg-st E was equal to the value calculated from the chemical formula. The magnesium contents of the other samples were higher than the theoretical value. Magnesium stearate is known to be mixed with magnesium palmitate, whose magnesium content is 4.14%. Because the magnesium content of most samples was larger than this, however, unreacted magnesium is thought to contaminate preparations of magnesium stearate.

The HPLC analysis of the fatty acid content of the various magnesium stearate samples showed several peaks other than those for stearic acid and palmitic acid. Because the sum of the other peak areas was less than 1% of the total of all peak areas, the other peaks were ignored and the contents of stearic acid and palmitic acid were calculated from their peak areas. The



TABLE 2

Properties of the various forms of magnesium stearate

Form	Particle size <sup>a</sup> ( $\mu\text{m}$ )	Specific surface area <sup>a</sup> ( $\text{m}^2 \text{g}^{-1}$ )	Bulk density ( $\text{g cm}^{-3}$ )	Moisture contents <sup>b</sup> (%)	Magnesium contents (%)	Palmitic acid/ stearic acid <sup>c</sup>
Mg-st A	2.74	2.04	0.139	5.19	4.91	30/70
Mg-st B	1.81	3.08	0.105	4.19	4.72	23/77
Mg-st C	1.27	4.39	0.126	5.90	4.56	32/68
Mg-st D	1.82	3.07	0.107	5.29	4.76	24/76
Mg-st E	1.18	4.73	0.068	6.95	4.11	30/70
Mg-st F	2.52	2.11	0.127	4.91	4.78	41/59

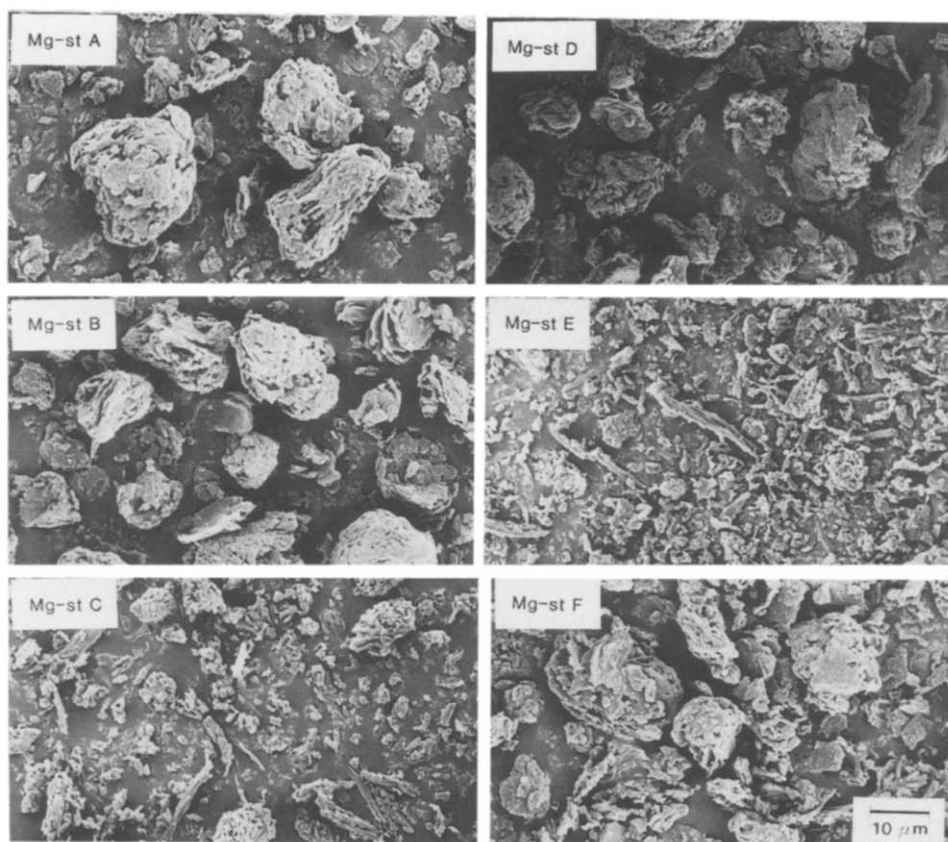
<sup>a</sup> By a Sub-Sieve Sizer, at 0.575 porosity.<sup>b</sup> By the Karl Fisher method.<sup>c</sup> By HPLC method for the determination of carboxylic acid using Br-DMEQ.

Fig. 4. Scanning electron micrographs of the various forms of magnesium stearate.

stearic acid content varied markedly from sample to sample, being in the range 57–77%. Palmitic acid was present in the range 23–41%. Thus, all the samples of magnesium stearate employed were mixtures of magnesium stearate and magnesium palmitate.

Particle size, specific surface area and bulk density were also determined for the various magnesium stearate samples and were found to vary markedly as indicated in Table 2. None of these physico-chemical properties of the various magnesium stearate samples could be correlated with the corresponding pattern of the DSC curve.

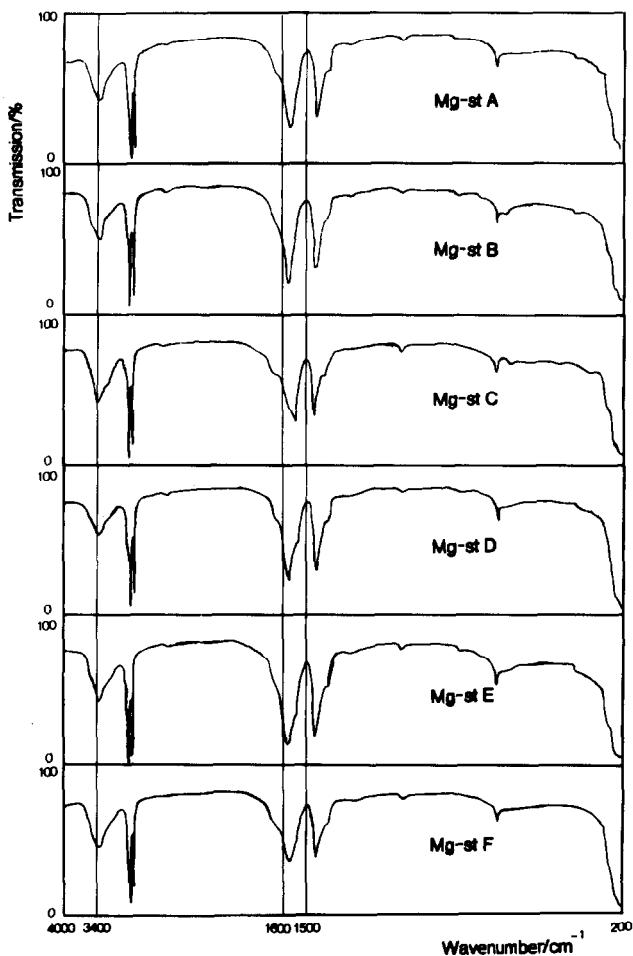


Fig. 5. IR spectra of the various forms of magnesium stearate.

### *Scanning electron microscopic observations of various magnesium stearate samples*

The samples of magnesium stearate were observed by SEM (Fig. 4). Crystals of Mg-st A, B, D and F are plate-shaped, while Mg-st E is needle-shaped. Mg-st C crystals are a mixture of plate and needle shapes. SEM observation also suggested that Mg-st C is a mixture of Mg-st B and E, as suggested by the DSC curve (Fig. 1). The results indicate no correlation of SEM data with the DSC curve patterns for the various magnesium stearate samples.

### *Observation of IR absorption spectra of magnesium stearate samples*

IR spectra of the various samples are shown in Fig. 5. All the samples, except for Mg-st C with a peak at  $1540\text{ cm}^{-1}$ , have an absorption at  $1580\text{ cm}^{-1}$ . Müller [15(a)] reported that one sample of magnesium stearate has a strong absorption peak at  $1540\text{ cm}^{-1}$  and a weak absorption peak at about  $3400\text{ cm}^{-1}$ . However, none of our samples showed absorption in this range. The IR spectra of magnesium stearate showed no correlation with the DSC curve patterns.

### *X-ray powder diffractograms of various magnesium stearate samples*

Figure 6 shows X-ray powder diffractograms of the various magnesium stearate samples. The X-ray diffractogram of Mg-st A is identical to that of

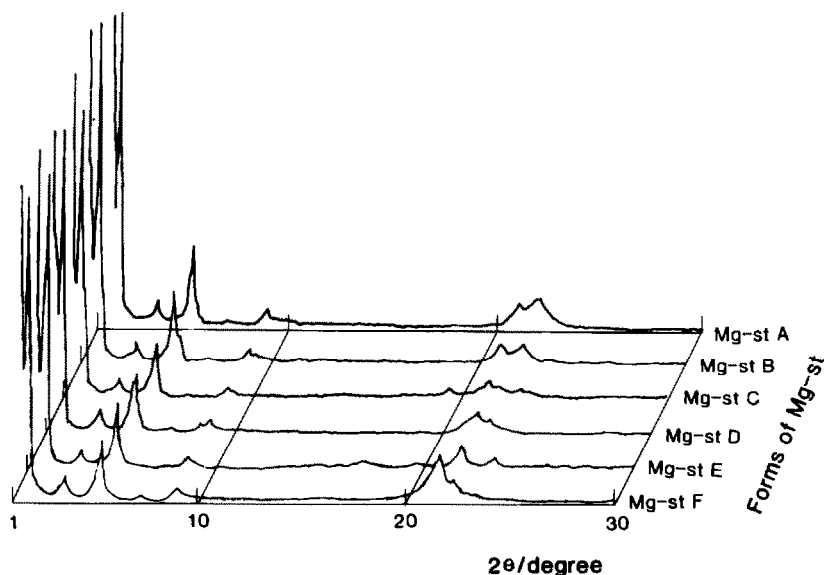


Fig. 6. X-ray powder diffractograms of the various forms of magnesium stearate.

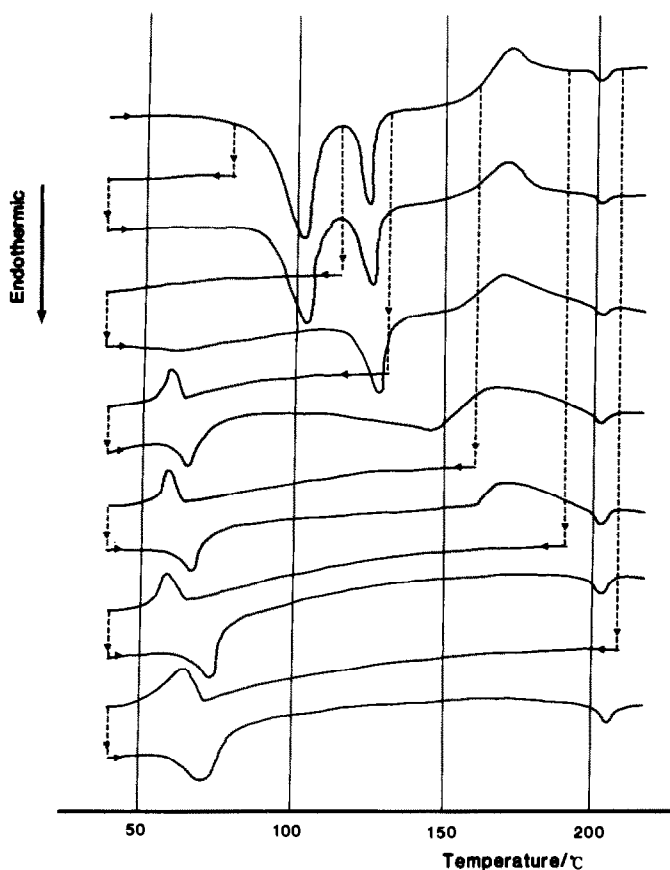


Fig. 7. DSC curves of Mg-st A for cooling and re-heating. After the samples were heated up to definite temperatures, they were measured when cooled from these temperatures to 37°C, and then on re-heating.

Mg-st B. The X-ray diffractogram of Mg-st D is similar to that of Mg-st A with an additional intensity at 5.040 deg. The X-ray diffractograms of Mg-st E and Mg-st F differ from each other and from the others.

The results shown in Fig. 6 indicate no relationship between the DSC pattern and the X-ray diffraction pattern of the magnesium stearate samples, although the X-ray powder diffractograms can indicate the presence of crystalline structures in a test compound.

#### *Effect of heating and cooling of magnesium stearate on its polymorphism*

Following heating of the samples to set temperatures, the DSC curves were measured during the cooling and re-heating processes (Fig. 7). The DSC curves of all samples show similar changes. The curves of the cooling process were taken as the base line when the sample was heated to just above the end-point temperature of the DSC peak associated with weight

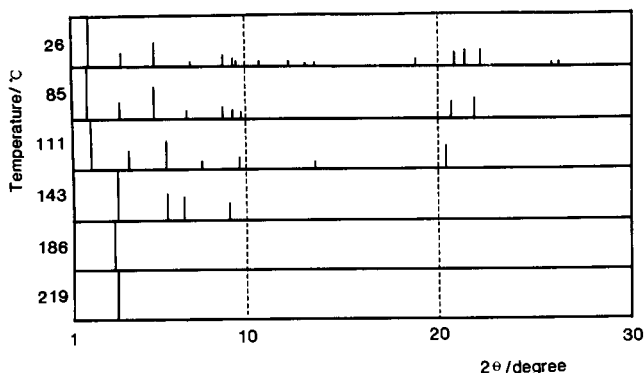


Fig. 8. X-ray powder diffraction patterns of Mg-st A at definite temperatures.

loss. The exothermic peak at about  $60^{\circ}\text{C}$  appeared when the sample was heated to just above the equivalent DSC peak without weight loss. When the sample was heated to just above the end-point temperature of the DSC peak with weight loss, the DSC curves in the re-heating process follow the base line until the temperature of the initial heating; then the curves have the same pattern as the initial curve above this point. When the sample was heated above the DSC peak temperature without weight loss, a broad endothermic peak appeared in the range  $68\text{--}78^{\circ}\text{C}$ ; then the curve fell from the peak to a stable state until the temperature of the previous heating was reached; the curves then were the same as the initial ones above this point. The exothermic peak or exothermic tendency observed at  $160\text{--}180^{\circ}\text{C}$  in samples Mg-st A, B, C and D disappeared, and only the DSC peak of Mg-st A at  $202^{\circ}\text{C}$  was detected again in the re-heating process.

The sample heated to a definite temperature was cooled rapidly by putting it on dry ice and storing it for 1 day. The DSC pattern in the re-heating process was measured and the peak in the  $68\text{--}78^{\circ}\text{C}$  range increased and shifted to a higher temperature, as is shown in Fig. 7.

X-ray powder diffractograms of Mg-st A were measured at temperatures just before and just after the DSC peak shown in Fig. 8.

The three intense peaks at  $2\theta = 21.20$ ,  $21.72$  and  $22.48$  deg observed in the diffractograms of Mg-st A at room temperature, became two peaks of  $2\theta = 20.88$  and  $22.08$  deg at  $85^{\circ}\text{C}$ , and one peak at  $2\theta = 20.34$  deg at  $111^{\circ}\text{C}$ . The peaks at around  $2\theta = 20$  deg disappeared at  $143^{\circ}\text{C}$ , whereas sharp peaks at  $3.32$ ,  $5.84$ ,  $6.72$  and  $9.00$  deg were detected at the same temperature. The peaks below  $10$  deg became  $3.02$  deg at  $186^{\circ}\text{C}$ , and  $3.16$  deg at  $219^{\circ}\text{C}$ . In addition, a broad peak at around  $18$  deg was detected in the diffractogram at temperatures above  $140^{\circ}\text{C}$ . Thus, a sharp peak in the range  $2.96\text{--}3.16$  deg and a broad peak at around  $18$  deg in the diffractogram were still present above the temperature of the meniscus point.

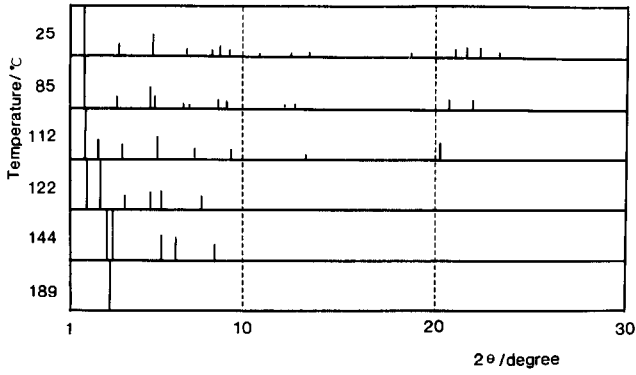


Fig. 9. X-ray powder diffraction patterns of Mg-st B at definite temperatures.

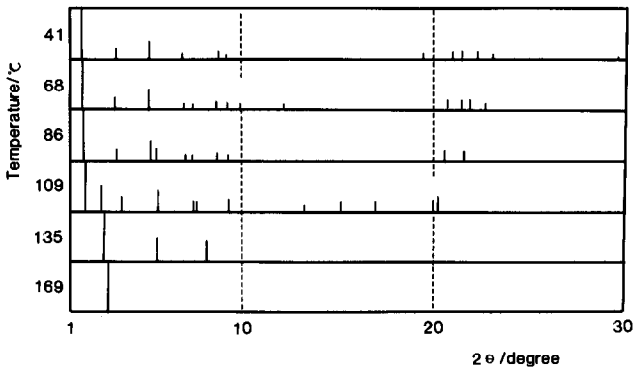


Fig. 10. X-ray powder diffraction patterns of Mg-st C at definite temperatures.

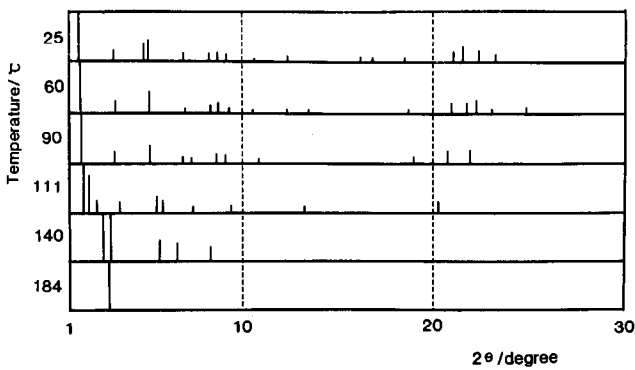


Fig. 11. X-ray powder diffraction patterns of Mg-st D at definite temperatures.

Figures 9–13 are the X-ray powder diffraction patterns of Mg-st B, C, D, E and F at definite temperature points. We examined the correlation between all the peaks in the diffractograms and the temperature and the

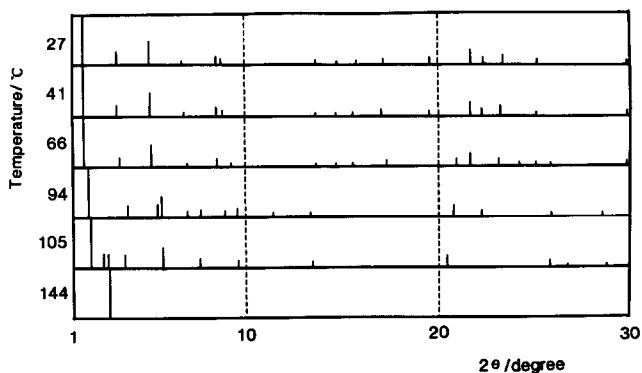


Fig. 12. X-ray powder diffraction patterns of Mg-st E at definite temperatures.

DSC peaks, but found no clear tendencies, except for some isolated findings. For example, similar peaks were seen in the X-ray diffractograms of Mg-st A at 111°C, Mg-st B at 112°C, Mg-st C at 109°C, Mg-st D at 111°C, Mg-st E at 105°C and Mg-st F at 110°C.

#### *Polymorphic behavior of magnesium stearate samples*

##### *DSC*

Magnesium stearate samples were treated as described in the Experimental section and their thermal properties were determined (Figs. 14–19). The washed samples of magnesium stearate showed DSC patterns fairly similar to those of the intact samples, except that a new DSC peak at about 65°C appeared in the washed Mg-st B. A drying treatment led to the disappearance of the peaks at about 65–80°C in Mg-st C, E and F.

When samples were stored at 60°C for 3 months (stored (1) in the figures), the DSC peaks at about 65–80°C disappeared or became weaker for the Mg-st C, D and F samples, while a DSC peak appeared at 144°C

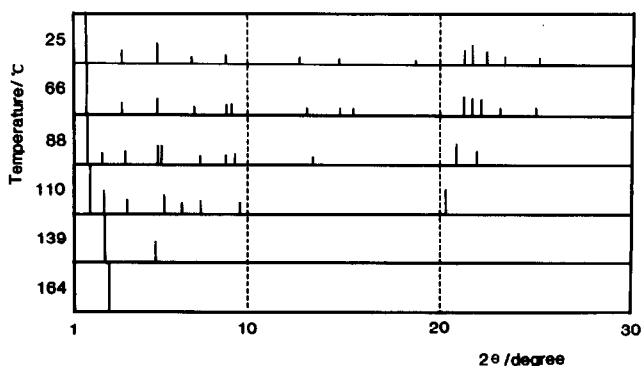


Fig. 13. X-ray powder diffraction patterns of Mg-st F at definite temperatures.

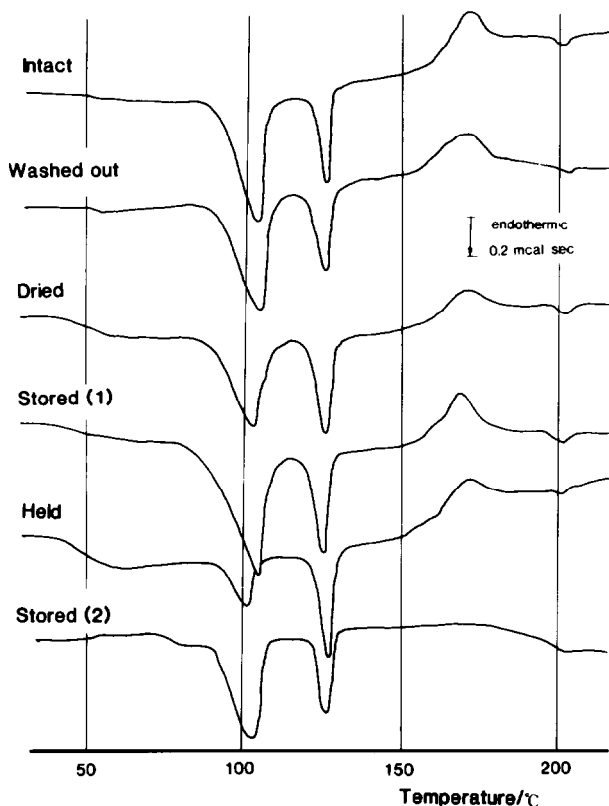


Fig. 14. DSC curves of Mg-st A derivatives. Washed, washed with acetone twice and kept at room temperature for 1 day to allow the acetone to vaporize; dried, dried in a reduced desiccator with phosphorous pentoxide for about 3 weeks; stored (1), stored at 60 °C for 3 months; held, held with the DSC set at 86 °C for 1 h; stored (2), stored in water at 60 °C for 1 month.

for Mg-st B. However, storage of magnesium stearate samples under wet conditions (stored (2) in the figures) resulted in the appearance or intensification of a DSC peak at about 65–80 °C in Mg-st B, C, D, E and F. These alterations in the DSC peak at 65–80 °C are thought to be due to moisture absorption or desorption. Maintaining Mg-st A and B at 86 °C caused no alterations in the DSC pattern, while maintaining Mg-st B at 86 °C under wet conditions (held (2) in Fig. 15) caused the appearance of a DSC peak at about 85 °C. The results support this.

As shown in Fig. 14, Mg-st A was found to be stable to heat, dryness and moisture. Although the DSC pattern of intact Mg-st B resembled that of Mg-st A, holding Mg-st B at 86 °C under wet conditions caused a change in the DSC pattern which matched the pattern of intact Mg-st D. The dried and stored (1) sample of Mg-st D showed a DSC pattern which was comparable to that of intact Mg-st B. This indicates the possible reversible transfer of magnesium stearate between Mg-st B and Mg-st D. However,



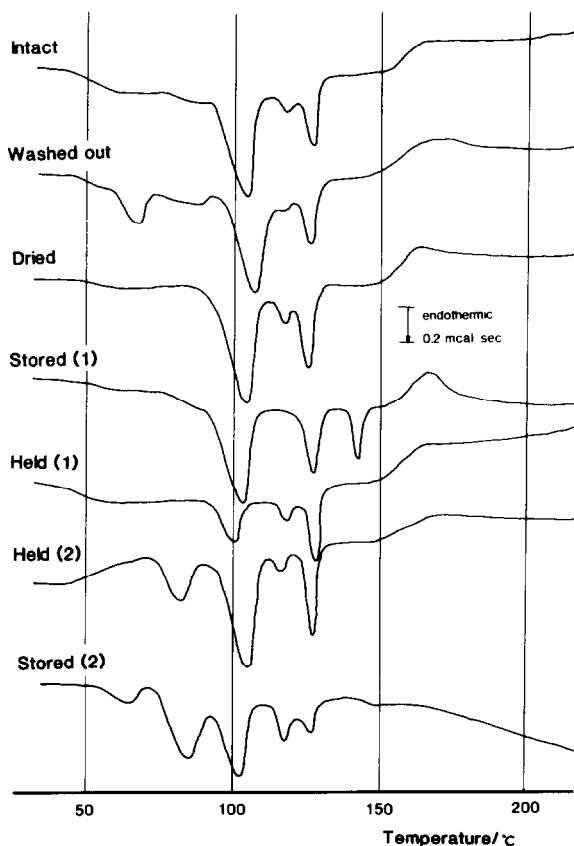


Fig. 15. DSC curves of Mg-st B derivatives. held (1), held with the DSC set at 86 °C for 1 h; held (2), held with the DSC set at 86 °C for 1 h with addition of water.

there was a small peak at about 140 °C for the stored (1) sample of Mg-st B, which cannot be explained. The crystalline transition of magnesium stearate samples between Mg-st D and F was observed from the comparable DSC patterns of stored (2) samples, although the DSC patterns of the intact samples differed markedly. A similarity in the DSC patterns was also detected in Mg-st E (stored (1)) and Mg-st F (stored (2)). The results of Figs. 14–19 show that the polymorphic behavior of magnesium stearate is probably controlled by both the heat and the adsorbed water molecules. Mg-st A was a stable sample showing no crystalline transition. Consequently, the polymorphic behavior of magnesium stearate has been defined as shown in Fig. 20.

### TG

As described previously, the TG–DSC curves of intact samples generally indicated one or several DSC peaks at lower temperatures, with weight loss due to the desorption of water, and one or several peaks at higher

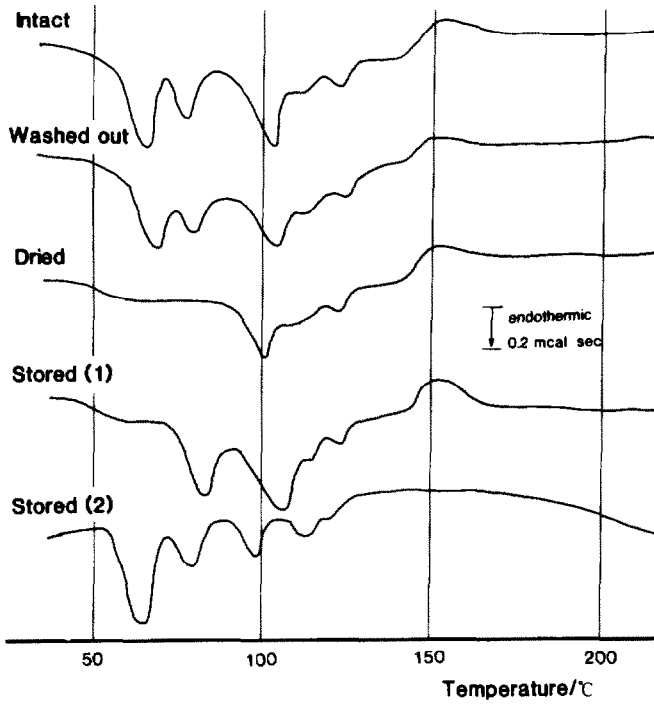


Fig. 16. DSC curves of Mg-st C derivatives.

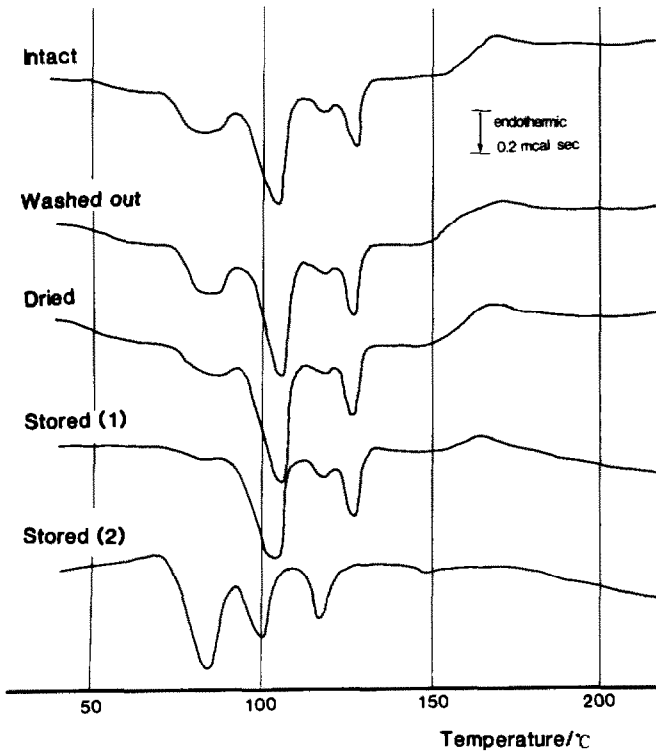


Fig. 17. DSC curves of Mg-st D derivatives.

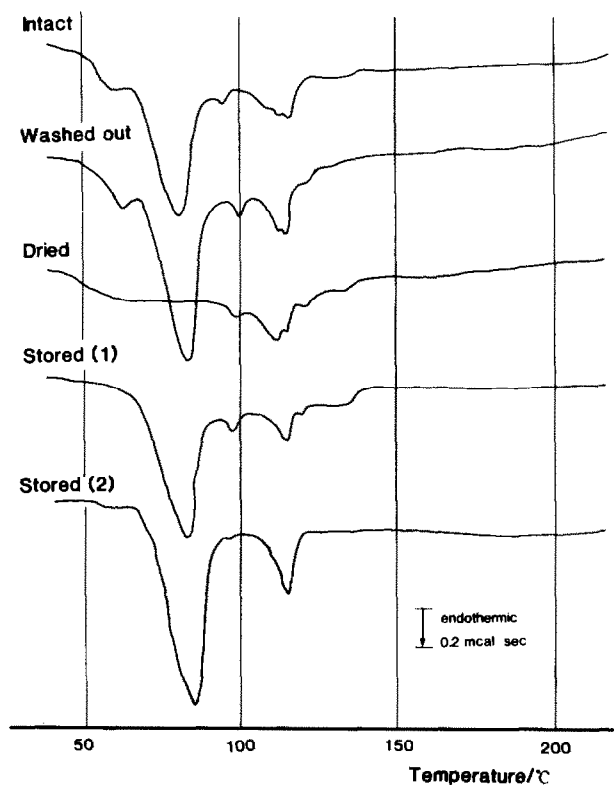


Fig. 18. DSC curves of Mg-st E derivatives.

temperatures without weight loss. The DSC curve of intact Mg-st F was an exception, having a peak at  $116^{\circ}\text{C}$  with weight loss of 0.09%. Similar phenomena were observed when magnesium stearate samples were treated as described in the Experimental section: the TG curve of the stored (1) sample of Mg-st B gave a stable line for the DSC peak at  $128^{\circ}\text{C}$ , but fell by 0.04% for the higher peak of  $142^{\circ}\text{C}$ . Similarly, the TG curve of the stored (2) sample of Mg-st B gave a stable line for the DSC peak at  $119^{\circ}\text{C}$ , but fell by 0.06% for the higher peak of  $127^{\circ}\text{C}$ . The TG curve of the stored (2) sample of Mg-st D also fell by 0.08% at the peak of  $128^{\circ}\text{C}$ . These were clear phenomena, but their mechanisms remain unexplained.

## CONCLUSIONS

Based on the above discussions, the following conclusions can be drawn.

1. Twenty-three batches of magnesium stearate were obtained from several suppliers, and their thermal properties were measured by DSC. The TG-DSC curves of the samples usually have one or several DSC peaks at lower temperatures with weight loss due to water desorption, and one or

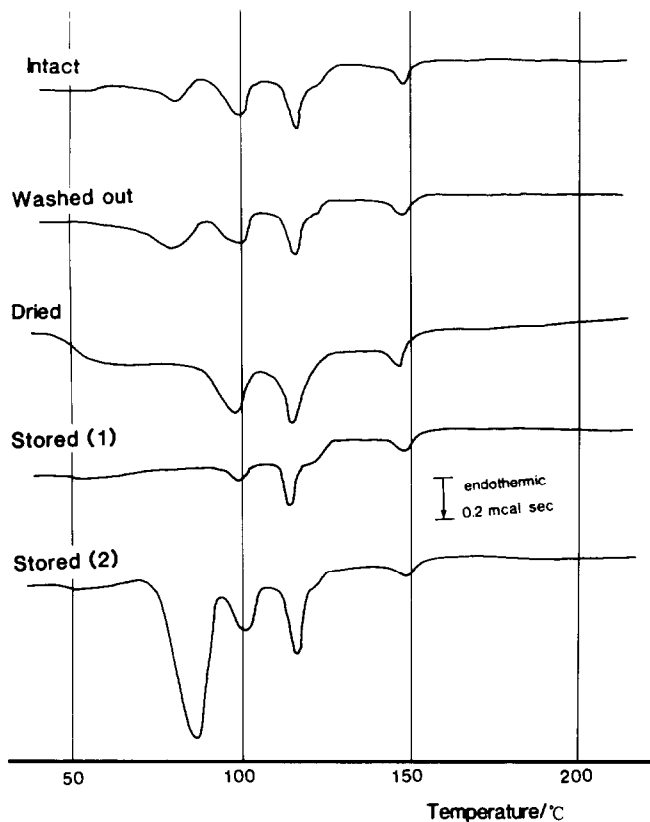


Fig. 19. DSC curves of Mg-st F derivatives.

several peaks at higher temperatures with stable weight. In addition, some samples showed an exothermic peak or exothermic phenomena with curves falling below the base line at about  $174^{\circ}\text{C}$  due to unreacted impurities.

2. The magnesium stearate samples examined were classified into six groups from their DSC curves. Scanning electron microscopy revealed crystalline forms of plate and/or needle shapes, but no correlation was found between the crystalline form and the DSC curves. Also, no correlation was found between the DSC curves and the physico-chemical properties of the samples.

3. X-ray powder diffractograms showed the existence of crystalline forms in all the magnesium stearate samples examined, although the various forms of magnesium stearate could not be distinguished by the diffractograms. Thus, the polymorphism of magnesium stearate samples could be detected by DSC, but not by X-ray diffractogram, infrared spectrum or electron microscopic observations.

4. The meniscus point of the magnesium stearate samples coincided approximately with the initial temperature of the DSC peak; this was supported by the X-ray results of the heated samples.

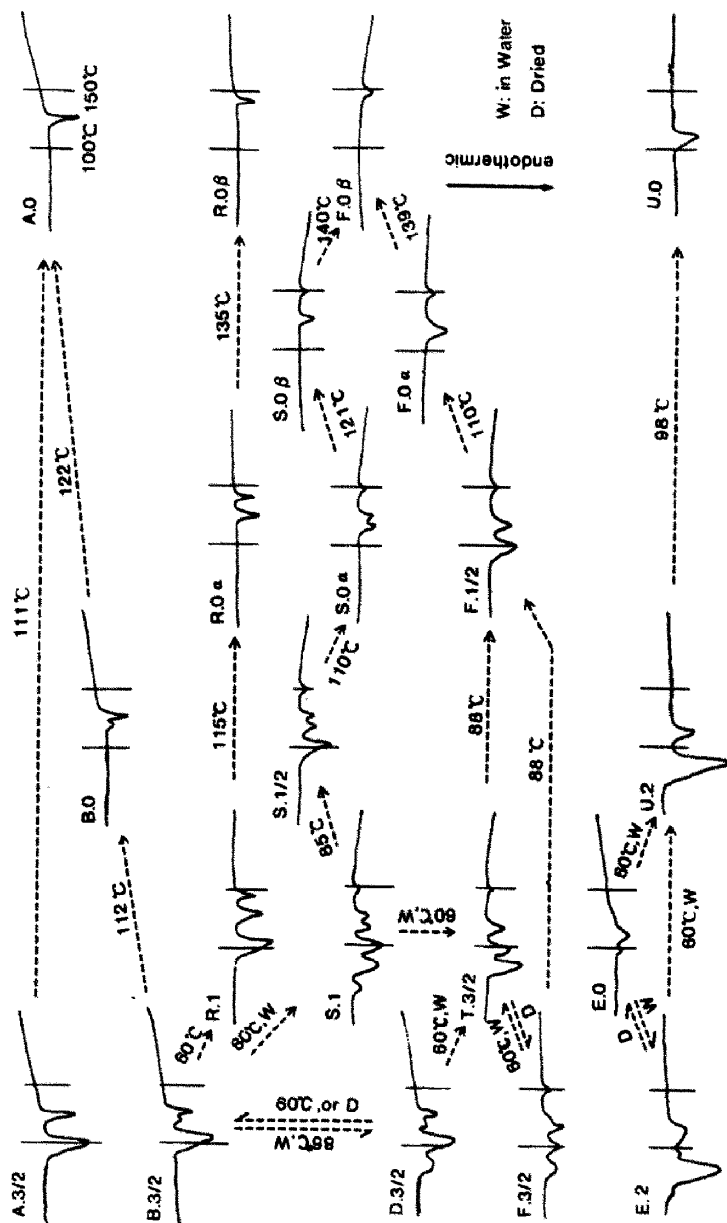


Fig. 20. The polymorphic behavior of magnesium stearate.

5. When the samples were stored at 86 °C with or without moisture, conversion of the DSC patterns was found, indicating transition of the crystalline form of magnesium stearate to another form. The crystal water is thought to play an important role in the transition.

#### ACKNOWLEDGMENTS

The authors thank Mr. M. Amamiya of Osaka Application Laboratories, Rigaku Corp. for his help with the X-ray powder diffraction studies, and Dr. T. Kitagawa, Dr. M. Takasuka, Dr. H. Kagawa, Mr. T. Takaoka, Mr. T. Matsuura, Mr. S. Nagata, Mr. T. Takemura, Ms. M. Sugita and Ms. K. Sakamoto in Shionogi Laboratories and Mr. Y. Sugita of the Division of Manufacture, Shionogi & Co., Ltd. for their help in running the analysis system and for their comments.

#### REFERENCES

- 1 H. Maekawa, T. Sakamoto and H. Takeda, *Yakkyoku*, 98 (1978) 1385.
- 2 P.V. Mroso, A.L.W. Po and W.J. Irwin, *J. Pharm. Sci.*, 71 (1982) 1096–1101.
- 3 J. Okada and Y. Hirai, *Yakugaku Zasshi*, 98 (1978) 1385–1390.
- 4 R.C. Rowe, *Int. J. Pharm.*, 41 (1988) 223–226.
- 5 A.C. Shah and A.R. Mlodozieniec, *J. Pharm. Sci.*, 66 (1977) 1377–1382.
- 6 J.G. Watt, *Int. J. Pharm.*, 36 (1987) 51–54.
- 7 S. Bolton and R. Atluri, *Drug Cosmet. Ind.*, 135 (1984) 44–50.
- 8 A.H. De Boer, G. Bolhuis and C.F. Lerk, *Powder Technol.*, 20 (1978) 75.
- 9 G. Ragnarsson, A.W. Holzer and J. Sjogren, *Int. J. Pharm.*, 3 (1979) 127–131.
- 10 W.A. Strickland, Jr., E. Nelson, L.W. Busse and T. Higuchi, *J. Am. Pharm. Assoc. Sci. Ed.*, 45 (1956) 51–55.
- 11 M. Ahmed and R.P. Enever, *Pharm. Acta Helv.*, 53 (1978) 358–364.
- 12 G. Levy and R.H. Gumtow, *J. Pharm. Sci.*, 52 (1963) 1139–1144.
- 13 T.A. Iranloye and E.L. Parrott, *J. Pharm. Sci.*, 67 (1978) 535–539.
- 14 D. Hansen, C. Führer and B. Schäfer, *Pharm. Ind.*, 32 (1970) 97–101.
- 15 (a) B.W. Müller, *Pharm. Ind.*, 38 (1976) 394–398.  
 (b) B.W. Müller, *Zentralbl. Pharm.*, 116 (1977) 1261–1266.  
 (c) B.W. Müller, *Pharm. Ind.*, 39 (1977) 161–165.  
 (d) B.W. Müller, K.J. Steffens and P.H. List, *Pharm. Ind.*, 44 (1982) 729–734.
- 16 K.J. Steffens, B.W. Müller and P.H. List, *Pharm. Ind.*, 44 (1982) 826–830.
- 17 T.A. Miller, P. York and T.M. Jones, *J. Pharm. Pharmacol.*, 34 Suppl. (1982) 8p.
- 18 I. Colombo and F. Carli, *Farmaco Ed. Prat.*, 39 (1984) 329–341.
- 19 R. Dansereau and G.E. Peck, *Drug Dev. Ind. Pharm.*, 13 (1987) 975–999.
- 20 (a) K.D. Ertel and J.T. Carstensen, *J. Pharm. Sci.*, 77 (1988) 625–629.  
 (b) K.D. Ertel and J.T. Carstensen *Int. J. Pharm.*, 42 (1988) 171–180.
- 21 U. Ikonen, H. Jalonen, E. Laine and K. Saaranivaara, *Acta Pharm. Fenn.*, 98 (1989) 137–138.
- 22 Y. Wada, E. Fukuoka and Y. Nakai, *Yakuzaigaku*, 50 (1990) 211–214.
- 23 Y. Suzuki, T. Takeda and K. Inazu, *Nihon Yakugakukai Youshi-syu*, 4 (1990) 102.
- 24 M. Yamaguchi, S. Hara, R. Matsunaga and M. Nakamura, *J. Chromatogr.*, 346 (1985) 227–236.